Autonomous role of medullary thymic epithelial cells in central CD4+ T cell tolerance

Ludger Klein, Maria Hinterberger, Martin Aichinger, Olivia Prazeres da Costa, David Voehringer, Reinhard Hoffmann

Autonomous role of medullary thymic epithelial cells in central CD4$^+$ T cell tolerance

Maria Hinterberger[1], Martin Aichinger[1], Olivia Prazeres da Costa[2], David Voehringer[1], Reinhard Hoffmann[2] and Ludger Klein[1]

[1] Institute for Immunology, Ludwig-Maximilians-University, Goethestr. 31, 80336 Munich, Germany

[2] Institute for Medical Microbiology, Immunology and Hygiene, Technical University Munich, Trogerstr. 30, 81675 Munich, Germany

Corresponding author is L.K. (ludger.klein@med.uni-muenchen.de)

Abstract

Medullary thymic epithelial cells (mTECs) serve an essential function in central tolerance through expressing peripheral tissue-antigens. These antigens may be transferred to and presented by dendritic cells. Therefore, it is unclear whether mTECs, besides being an 'antigen reservoir', also serve a mandatory function as antigen presenting cells. Here, we reduced major histocompatibility complex class II on mTECs through transgenic expression of a C2TA-specific 'designer miRNA'. This resulted in an enlarged polyclonal CD4 single-positive compartment and, among thymocytes specific for model-antigens expressed in mTECs, enhanced selection of regulatory T cells (T_{reg}) at the expense of deletion. Our data document an autonomous contribution of mTECs to both dominant and recessive mechanisms of CD4 T cell tolerance and support an avidity model of T_{reg} development versus deletion.

Introduction

Hematopoietic and epithelial stromal cells in the thymic medulla establish a unique microenvironment that is essential for the generation of a self-tolerant T cell repertoire [1-2]. However, the precise qualitative and quantitative contribution of individual thymic stromal cell subsets to distinct modes of central T cell tolerance, for instance, negative selection versus deviation into the Foxp3$^+$ regulatory T (T_{reg}) cell lineage, has not been clarified.

Traditionally, deletion of autoreactive CD4 single-positive (SP) thymocytes has largely been attributed to the antigen presenting cell (APC) function of thymic dendritic cells (DCs). Elimination of major histocompatibility complex (MHC) class II expression on hematopoietic cells or, more recently, genetic ablation of DCs, increased the number of CD4SP thymocytes by 30 – 60 % [3-4]. This has been interpreted to reveal the contribution of antigen recognition on DCs to negative selection of CD4$^+$ T cells. Whether the second major subset of stromal cells in the medulla, that is, medullary thymic epithelial cells (mTECs), has a crucial APC function remains to be established. It is undisputed that mTECs as such serve an essential role for central tolerance – for instance, a developmental block in the mTEC lineage through interference with the NF-kappaB signaling axis results in autoimmunity [5-10]. However, the interpretation of these observations remains complex because perturbations of mTEC differentiation do not only affect their *bona fide* APC function, but may also disrupt the three-dimensional organization of the medulla and diminish the phenomenon of 'promiscuous' expression of peripheral tissue-antigens (PTAs). PTA expression is to a substantial degree under the control of the autoimmune regulator (*Aire*) gene [11-12], whose expression is largely confined to terminally differentiated mTECs [13], and by itself is indispensable to prevent

autoimmunity [14]. Therefore, self-tolerance failure caused by defective mTEC differentiation may reflect their role as 'PTA reservoir' rather than any autonomous APC function.

The 'antigen reservoir' scenario is supported by a model system in which negative selection of $CD4^+$ T cells specific for an mTEC-derived antigen was strictly dependent on antigen presentation by hematopoietic APCs, most likely DCs [15]. Such 'spreading' of antigens or even intact MHC molecules from mTECs to DCs may be a common occurrence [16-17], possibly facilitated through an alleged pro-apoptotic function of Aire [18]. In support of an autonomous APC function of mTECs, transgenic hemagglutinin (HA)-expression in mTECs was found to promote the differentiation of specific $CD4^+$ T cells into the T_{reg} cell lineage through direct antigen recognition on HA-expressing and –presenting mTECs [19]. Along these lines, the terminal differentiation of mTECs not only coincides with the onset of promiscuous gene expression, but also with the acquisition of a surface phenotype (MHC class II^{hi} $CD80^{hi}$) that is suggestive of potent APC capacity.

Intriguingly, in studies that characterized the contribution of DCs versus mTECs in tolerance towards mTEC-derived antigens, cross-presentation by DCs or autonomous presentation by mTECs resulted in a partly different mode of $CD4^+$ T cell tolerance, that is, negative selection versus T_{reg} induction, respectively [15, 19]. A significant number of variables (TCR, antigen, topology and level of antigen expression) exist between the models used, so these studies do not necessarily indicate that qualitative differences between mTECs and DCs impose distinct mechanisms of tolerance. Instead, these observations are also compatible with a model of thymocyte fate specification according to which T_{reg} differentiation occurs within an avidity window between positive selection and deletion [20-21]. Importantly, the

avidity hypothesis entails a testable prediction: under given conditions (i.e., fixed TCR and APC), reducing the avidity of antigen recognition should diminish clonal deletion and favor T_{reg} induction within a specific cohort of MHC class II restricted thymocytes.

Here, we addressed the autonomous APC function of mTECs by interfering with MHC class II-restricted antigen presentation while preserving their 'antigen reservoir' function. Conditional ablation of MHC class II expression may appear to be suitable to address this question. However, because MHC class II dependent cognate interactions between thymocytes and mTECs have been implicated in mTEC homeostasis and maturation [22], the complete elimination of MHC class II could possibly perturb mTEC development and hence blur a clear dissociation of their APC- from their 'antigen reservoir'-function. Therefore we pursued a strategy that reduced, but not fully eliminated, MHC class II on mTECs. This strategy also allowed testing the central prediction of the avidity model of T_{reg} differentiation. To do so, we devised a transgenic system in which MHC class II expression is diminished through tissue-specific expression of a 'designer' micro (mi)RNA which silences C2TA (class 2 transactivator), the master regulator of MHC class II expression [23].

Results

'Designer' miRNA mediated silencing of C2TA *in vitro*

Synthetic small hairpin RNA (shRNA) sequences integrated into the miRNA-30 backbone are processed by the miRNA machinery and can be used for gene silencing [24]. Unlike 'naked' short hairpins, whose transcription requires RNA Polymerase III (Pol III) promoters, transcription of such 'designer' miRNAs is driven

by Pol II promoters, thus offering the potential for tissue-specific or temporally controlled gene silencing *in vivo* [25-26].

Following this strategy, several shRNA sequences (see **Methods** for details of sequence selection) complementary to C2TA were cloned into the retroviral vector MSCV-LTRmiR30-PIG (LMP) [27]. In these constructs, the synthetic shRNA is embedded in the pri-miRNA-30 backbone, replacing the physiologically processed miRNA-30 hairpin structure (**Fig.1a**) [27-28]. To assess C2TA silencing, MHC class II expression was determined by flow cytometry and Western analysis in LMP infected WEHI 279.1 cells. One construct, designated C2TAsh(6) (**Fig. 1a,b**), consistently mediated the most efficient MHC class II reduction (**Fig. 1c,d**) and was therefore chosen for further experiments.

mTEC-specific silencing of C2TA in transgenic mice

To silence C2TA specifically in mTECs, we generated a bacterial artificial chromosome (BAC) transgene in which the start codon of *Aire* was replaced by the C2TA-specific miRNA construct C2TAsh(6) (**Fig. 2a**). Of two individual founder lines that had essentially identical phenotypes in preliminary analyses, one (referred to as 'C2TAkd') was chosen for detailed analyses.

First, we assessed the faithful tissue specificity and proper processing of the C2TAkd transgene. To facilitate the phenotypic distinction of mTEC subsets, we crossed C2TAkd mice with AIRE-reporter (Adig) mice, in which green fluorescent protein (GFP) is expressed from a modified *Aire* locus [29]. We analyzed the abundance of the properly processed C2TAkd miRNA and of the *Aire* mRNA in purified thymic stromal cells using a custom miRNA TaqMan assay or quantitative RT-PCR, respectively. The two RNA species tightly correlated. Specifically, both transcripts were most

abundant in the 'mature' ($CD80^{hi}$Aire-GFP^{+}) subset of mTECs, were detectable at about three-fold lower expression levels in $CD80^{hi}$Aire-GFP^{-} mTECs, and were hardly expressed in 'immature' ($CD80^{lo}$Aire-GFP^{-}) mTECs (**Fig. 2b,c**).

Next, we used quantitative RT-PCR to asses whether the mRNA abundance of *Ciita* and of a representative C2TA target, *H2-Aa*, were altered in C2TAkd mTECs. In wild-type controls, *Ciita* and *H2-Aa* mRNA levels positively correlated with mTEC maturation, that is, both transcripts increased from $CD80^{lo}AIRE^{-}$ to $CD80^{hi}AIRE^{-}$ cells and had the highest expression in $CD80^{hi}AIRE^{+}$ mTECs. By contrast, this progressive up-regulation of *Ciita* and *H2-Aa* mRNA was abolished in C2TAkd mice (**Fig. 3a**). Microarray expression profiling of C2TA target genes in $CD80^{hi}$ mTECs revealed a significant down-regulation of all MHC class II subunits and of several accessory molecules of the MHC class II pathway (**Fig. 3b**). For comparison, we also included $Ciita^{-/-}$ mTECs, which expectedly displayed a more pronounced reduction of C2TA target gene expression (**Fig. 3b**). Consistent with MHC class I expression being largely C2TA independent [30], expression of MHC class I genes was not affected in C2TAkd or $Ciita^{-/-}$ mice (**Fig. 3c**). Likewise, several MHC class II-unrelated and controversially discussed putative targets of C2TA [31] were expressed at identical levels in C2TAkd, $Ciita^{-/-}$ and wild-type mTECs (**Fig. 3c**), supporting the view that these genes may not at all or only indirectly be influenced by C2TA [30]. Collectively, these data established the faithful tissue-specificity, proper processing and functionality of the 'designer' miRNA transgene.

Phenotype and APC-function of C2TAkd mTECs

Flow cytometric analyses revealed a marked reduction of MHC class II on 'mature' $CD80^{hi}$ mTECs from C2TAkd mice (**Fig. 4a**). 'Immature' $CD80^{lo}$ mTECs of wild-type

animals are characterized by relatively low MHC class II surface expression, which was further reduced in C2TAkd mice. cTECs as well as three subsets of thymic DCs [32] (Sirpα^{-} 'autochthonous' DCs, Sirpα^{+} 'migratory' DCs and plasmacytoid DCs) displayed MHC class II levels identical to wild-type controls (**Fig. 4a**), confirming the absence of transgene expression in stromal cells other than mTECs. Quantitative Western analysis of a representative MHC class II component, H2-Ea, demonstrated a ten-fold reduction in 'mature' C2TAkd mTECs (**Fig. 4b**). Consistent with our mRNA and FACS data, no differences in H2-Ea protein expression were seen in CD11c^{hi} DCs (**Fig. 4b**). Low MHC class II on C2TAkd mTECs correlated with their reduced capacity to present peptide antigen to MHC class II-restricted T cells *in vitro*. In the presence of titrated amounts of peptide, purified C2TAkd mTECs required approximately ten-fold more antigen to elicit a response equivalent to wild-type cells in antigen specific CD4^{+} T cell hybridoma cells (**Fig. 4c**).

Cognate interactions between CD4SP thymocytes and MHC class II on mTECs were suggested to coordinate the differentiation and homeostasis of 'mature' mTECs [22]. However, the abundance of CD80^{hi} mTECs (**Supplementary Fig. 1**) and the frequency of the 'most mature' (AIRE^{+}) mTECs, which represent a subset of CD80^{hi} cells, was identical in C2TAkd and wild-type mice (**Fig. 4d**). In addition, histological examination showed that C2TAkd thymi were properly organized into cortical and medullary regions (**Supplementary Fig. 2**) in which AIRE^{+} mTECs were normally distributed (**Fig. 4e**). Lastly, the 'promiscuous' expression of several representative Aire-dependent and Aire-independent PTAs was indistinguishable between C2TAkd and wild-type mTECs (**Fig. 4f**). These results indicate that the degree of MHC class II reduction achieved in C2TAkd mTECs does not interfere with their normal development.

Together, these observations show that C2TA silencing causes a considerable diminution of MHC class II in mTECs. The alteration of MHC class II surface expression exceeds that of individual C2TA-dependent mRNAs related to the MHC class II pathway, suggesting that additive effects amplify the degree of MHC class II reduction. This manipulation diminishes the capacity of mTECs to present antigen to $CD4^+$ T cells, but does not perturb differentiation and organization of the medullary compartment and leaves the phenomenon of PTA expression intact.

Enlarged CD4SP compartment in C2TAkd mice

C2TAkd mice were viable and did not show overt signs of autoimmunity. Histological examination revealed a moderately elevated incidence of sporadic lymphocyte infiltrations in several organs of C2TAkd as compared to wild-type animals (**Supplementary Fig. 3**), yet without consistent involvement of a particular target organ.

We next asked whether C2TA silencing in mTECs had an impact on polyclonal thymocyte development. Flow cytometry revealed a significantly enlarged CD4SP compartment in C2TAkd thymi as compared to wild-type controls (**Fig. 5a,b**), and the frequency of $Foxp3^+$ T_{reg} cells among CD4SP thymocytes was slightly elevated (5.7 ± 1.4 % versus 3.9 ± 0.9 % (n = 9); $P = 0.004$). By contrast, no change was seen in the abundance of CD8SP cells (**Fig. 5b**). The increased CD4SP compartment in C2TAkd thymi might reflect the escape of CD4SP thymocytes from clonal deletion due to diminished MHC class II-restricted presentation of autoantigens by mTECs.

Because the enlarged CD4SP compartment in C2TAkd thymi was reminiscent of earlier studies addressing the quantitative impact of DCs on negative selection of $CD4^+$ T cells [3-4], we directly compared the contribution of hematopoietic APCs and

radioresistant mTECs in a set of bone marrow chimeras (**Fig. 5c,d**). Compared to thymi of wild-type into wild-type control chimeras, both wild-type into C2TAkd as well as *H2-Ab1*$^{-/-}$ (MHCII-KO*)* into wild-type chimeras harbored a significantly enlarged CD4SP compartment. Combining hematopoietic MHC class II deficiency with MHC class II reduction on mTECs in MHCII-KO into C2TAkd chimeras resulted in the most pronounced increase in CD4SP cells, suggesting an additive, non-redundant contribution of DCs and mTECs to negative selection of MHC class II-restricted thymocytes. The fraction of Foxp3$^+$ T_{reg} cells among CD4SP cells in the different chimeras was not significantly different; however, there was a tendency towards an increased fraction of Foxp3$^+$ cells among CD4SP thymocytes in WT→C2TAkd BM chimeras (data not shown). Collectively, these data suggest that mTECs substantially contribute to deletional CD4$^+$ T cell tolerance through directly acting as APCs. Also, they support the idea that DCs and mTECs mediate clonal deletion of distinct spectra of MHC class II-restricted TCR specificities.

Altered fate of autoreactive CD4$^+$ T cells

The described experiments did not address the antigen specificity or the fate of cells that presumably evaded central tolerance induction in C2TAkd mice. In addition, the tissue-specificity and expression levels of the endogenous tolerogenic self-antigens were not adequately evaluated. We therefore followed the developmental fate of MHC class II-restricted thymocytes of known antigen specificity. We used two previously established neo-self antigen transgenic model systems where cognate epitopes of ovalbumin (OVA) or hemagglutinin (HA) are expressed specifically in mTECs [19].

In Aire-OVA mice, a fusion protein containing the OVA(323–339) epitope recognized by the DO11.10 TCR is specifically expressed in mTECs from an *Aire*-BAC transgene. In DO11.10 x AIRE–OVA double-transgenic mice two thirds of DO11.10$^+$ CD4SP cells are deleted concomitant with a considerable increase in Foxp3$^+$ T_{reg} cells among the remaining OVA-specific thymocytes [19]. We verified that the introduction of the C2TAkd transgene into the Aire-OVA system did not alter the level and tissue-specificity of antigen expression (**Fig. 6a**). We also established that in the absence of cognate antigen positive selection of DO11.10$^+$ thymocytes was indistinguishable in DO11.10 × C2TAkd versus DO11.10 mice (**Fig. 6b**). In the presence of cognate antigen expression, however, silencing of C2TA profoundly altered the fate of DO11.10$^+$ thymocytes. First, the loss of OVA-specific cells was strongly diminished in DO11.10 × Aire-OVA × C2TAkd mice (**Fig. 6b,c**). Second, DO11.10 × Aire-OVA × C2TAkd thymi not only contained a significantly higher number of OVA-specific CD4SP cells with an apparently 'naïve' Foxp3$^-$ phenotype, but also harbored a significantly increased frequency and absolute number of DO11.10$^+$ T_{reg} cells (**Fig. 6d–f**).

To ask whether these findings could be reproduced in a related model of different antigen specificity, we examined the consequences of mTEC-specific C2TA silencing in TCR-HA × Aire-HA mice. This model, in which CD4SP cells recognize the HA(107-119) epitope, is very similar to the DO11.10 × Aire-OVA model. Expression of HA exclusively in mTECs was sufficient for the differentiation of a considerable fraction of specific CD4SP cells into the T_{reg} cell lineage, but also lead to a substantial loss of TCR-HA$^+$ thymocytes (**Fig. 7a**) [19]. Silencing of C2TA through the introduction of the C2TAkd transgene reduced the extent of clonal deletion of TCR-HA$^+$ cells (**Fig. 7a,b**) and at the same time led to the emergence of a significantly higher number of T_{reg}

cells (**Fig. 7c–e**). A third system, the TCR-HA × Pgk-HA model [33], where expression of HA is driven by the ubiquitous phosphoglycerate kinase (*Pgk1*) promoter, yielded similar results (**Supplementary Fig. 4**). Collectively, these findings bolster the idea that reducing the avidity of autoantigen-recognition on mTECs can result in the escape of autoreactive $CD4^+$ T cells from clonal deletion. Because this 'rescue' from clonal deletion coincides with an increased emergence of antigen specific T_{reg} cells, these data also provide support for an avidity model of deletion versus T_{reg} differentiation.

mTECs induce clonal deletion and T_{reg} differentiation

Antigens expressed by mTECs may be transferred to and presented by thymic DCs [15, 17]. We therefore considered that the complex changes in the fate of autoreactive $CD4^+$ T cells caused by silencing of C2TA in mTECs may have been partially caused by alterations in the relative contribution of mTECs versus 'cross-presenting' DCs. The contribution of intercellular antigen transfer to central tolerance induction was previously addressed in bone marrow chimeras with MHC-deficient or -mismatched hematopoietic compartments [15, 19]. Because 'spreading' of self-determinants from mTECs to DCs not only applies to protein antigens, but also to functional MHC molecules [16], the transfer of peptide loaded MHC molecules to DCs remains a confounding issue in such chimeras. To circumvent this caveat, we used bone marrow from mice expressing diphteria toxin in $CD11c^+$ cells ('ΔDC' mice) [3]. Analysis of chimeric Aire-OVA mice reconstituted with DO11.10 or DO11.10 × ΔDC bone marrow revealed an identical phenotype of OVA-specific thymocytes in both groups (**Fig. 8a**), indicating that neither the partial deletion nor the concomitant T_{reg} induction in this model required the physical presence of DCs.

We combined DC-deficiency with mTEC-specific silencing of C2TA by reconstitution of Aire-OVA × C2TAkd recipients with DO11.10 × ΔDC bone marrow. In this setting, the 'rescue' of DO11.10$^+$ thymocytes from negative selection was very profound (**Fig. 8a**) and coincided with a significantly higher frequency and absolute number of DO11.10$^+$ thymoctes that differentiated into Foxp3$^+$ T_{reg} cells (**Fig. 8b,c**) or emerged as apparently naïve Foxp3$^-$cells (**Fig. 8d**).

These findings were confirmed in the Aire-HA model (**Supplementary Fig. 5**). Thymocyte subset composition and phenotype were identical in Aire-HA hosts reconstituted with TCR-HA or TCR-HA × ΔDC bone marrow. Irrespective of a potential contribution of DCs, the C2TAkd transgene decreased the negative selection of TCR-HA$^+$ cells and increased the selection of TCR-HA$^+$ T_{reg} cells. In sum, these data strongly support the notion that both the decreased negative selection and the increased T_{reg} induction resulting from mTEC-specific C2TA silencing ensue from an attenuation of the autonomous APC function of mTECs through diminution of their MHC class II levels and exclude an indirect contribution from DCs.

Discussion

Our findings illustrate the feasibility and value of the transgenic silencing approach in the context of qualitative and also quantitative aspects of a biological question. Using a strategy that diminished instead of entirely abolished MHC class II expression on mTECs, we avoided effects of MHC class II deletion on the composition or functional properties of the mTEC compartment [22] and we could test the hypothesis that cell fate decisions of autoreactive CD4$^+$ T cells are imprinted by the avidity of cognate antigen encounter.

Effects of C2TA silencing on target genes not immediately involved in MHC class II-restricted antigen presentation or potential off-target effects of the 'designer' miRNA cannot be formally excluded. However, considering the consistency of our observations we think these effects are highly unlikely. Collectively, our data demonstrate several key aspects of the DC-independent contribution of mTECs to central $CD4^+$ T cell tolerance.

First, deletion of polyclonal thymocytes resulting from cognate interactions with mTECs, when compared to the corresponding role of DCs, is clearly not a 'minority phenomenon'. Since our strategy did not entirely eliminate MHC class II from mTECs, but reduced its surface density to approximately 10 % of wild-type levels, it is likely that this approach underestimates the full extent of mTEC-mediated deletion of $CD4^+$ T cells. These considerations may explain why selective attenuation of antigen presentation by mTECs only resulted in a sporadic incidence of mild tissue infiltrations, whereas defective mTEC development – affecting both their 'antigen reservoir' and APC function – led to spontaneous autoimmunity [5-10]. These results could be interpreted as an indication that antigen presentation by mTECs is not truly essential to prevent autoimmunity. However, the residual MHC class II expression in C2TAkd mice might still suffice to censor autoreactive $CD4^+$ T cells at the very high end of the affinity spectrum. 'Escape' of such cells may be a critical event in the etiology of spontaneous autoimmunity. It should be noted that lack of Aire, which selectively abolishes the 'antigen reservoir' function of mTECs (as far as the Aire dependent set of PTAs is concerned), does not quantitatively alter the thymocyte subset distribution, but leads to spontaneous autoimmunity, whereas C2TA silencing promotes an inverse outcome. Given the complex interplay of dominant and recessive modes of central tolerance, future work is needed to globally characterize

the impact of Aire deletion as compared to silencing of MHC class II on a polyclonal T cell repertoire. Large scale sequencing of thymic naïve and T_{reg} repertoires may represent one approach.

Second, our data support the view that there is a significant degree of non-overlap between the spectra of autoantigen-derived MHC class II-bound epitopes presented by mTECs and DCs [2]. This becomes particularly evident from the additive effects of MHC class II-ablation in DCs and C2TA silencing in mTECs on the size of the polyclonal CD4SP compartment. This non-redundancy most likely relates to differences in the way these cells sample antigens presented by MHC class II. Thus, DCs predominantly select epitopes generated through classical, exogenous MHC class II loading, whereas MHC class II-bound peptides on mTECs may at least in part originate from unconventional, endogenous MHC class II loading [2, 17, 34-36]. The unexpectedly large contribution of peripheral, migratory DCs to the thymic DC pool [37-38] adds a further layer of complexity to such a 'division-of-labor' among thymic stromal cells. Whether $CD4^+$ T cell tolerance towards a particular mTEC-derived antigen requires transfer to and presentation by thymic DCs may be influenced by the frequency of expressing mTECs, the amount of antigen expressed by individual mTECs or the sub-cellular localization of the respective antigen.

Third, using TCR transgenic models we characterized the modalities of antigen recognition that may favor negative selection or T_{reg} differentiation. In both transgenic systems analyzed, DC ablation had minimal if any bearing on the fate of $CD4^+$ T cells specific for mTEC-derived antigens, substantiating the notion that antigen recognition on mTECs can promote both deletion and T_{reg} development [19]. Other stromal APCs have been implicated in shaping of the T_{reg} repertoire [38-42], and it is conceivable that DCs and also cortical TECs may have a similar dual function. By inference, variables

other than particular qualities of the APC itself may specify deletion versus T_{reg} differentiation. The functional avidity of the cognate interaction is a prime candidate. Indeed, our observations are consistent with a central prediction of this 'avidity hypothesis'. Attenuation of MHC class II restricted antigen presentation by mTECs, while (i) preserving the level and tissue-specificity of antigen expression, (ii) keeping the responding thymocyte population identical and (iii) excluding potential 'cross-presentation' by DCs, diminished the efficacy of negative selection in two TCR transgenic models and led to the increased emergence of T_{reg} cells.

Finally, there are several explanations for the relatively minor increase of the polyclonal T_{reg} pool in C2TAkd mice. In view of the 'avidity hypothesis', it is conceivable that the T_{reg} conversion of TCR specificities that would normally be negatively selected might be compensated by the 'escape' of *bona fide* T_{reg} cells as naïve cells. However, a model solely based on avidity is certainly an over-simplification [21]. Thus, the size of the T_{reg} cell pool is not just a reflection of the number of precursors carrying a 'matching' TCR, but is also controlled by additional factors. On the one hand, antigen-unspecific environmental cues have a role, as T_{reg} differentiation is known to segregate into a TCR-driven instructive phase and a cytokine-dependent 'consolidation' phase ('two-step model') [43]. On the other hand, intraclonal competition, possibly caused by limited access to antigen, restricts the number of clonal precursors that actually enter the T_{reg} lineage [44-45]. In this context, it is intriguing to note that the presentation of certain PTAs, due to stochastic fluctuations in 'promiscuous' gene expression, may be restricted to a very limited number of stromal APCs [46-47].

Accession Codes

Microarray data have been submitted to the GEO database (Accession number GSE20276).

Acknowledgements

We thank B. Kyewski (German Cancer Research Center) for critical reading of the manuscript, and C. Federle and S. Hoeflinger for expert technical assistance. M.S. Anderson (University of California San Francisco), K. Karjalainen (Nanyang Technological University) and H.S. Scott (University of Adelaide) kindly provided mice or reagents. Work in the lab of L.K. is supported through grants from the Deutsche Forschungsgemeinschaft (KL 1228/3-1 to L.K. and M.H.; SFB 455 to L.K. and M.A.). This work was also supported by the Austrian National Science Fund (FWF) (SFB23). D.V. receives support from the Emmy-Noether program of the Deutsche Forschungsgemeinschaft (VO 944/2-2).

Author contributions

M.H. generated and analyzed the C2TAkd model as well as the compound transgenic mice and bone marrow chimeras. M.H. was also involved in essentially all other experiments. M.A. carried out the expression analyses by quantitative PCR. O.P.C. and R.H. performed microarray experiments. D.V. provided ΔDC mice. L.K. and M.H. designed experimental strategies and wrote the manuscript.

Competing financial interest

The authors declare no competing financial interest.

Figure Legends

Fig. 1 Reduced MHC class II expression through C2TA silencing *in vitro*. (**a**) Schematic representation of the miRNA-30 backbone in the retroviral vector MSCV-LMP modified to encode for several synthetic hairpin sequences complementary to the coding region of the C2TA mRNA. Sequence details of one such construct, C2TAsh(6), are depicted underneath the vector diagram, with sequences of the predicted mature 'designer' miRNA underlined. (**b**) Alignment of the C2TAsh(6) leading strand (antisense) with the three C2TA mRNA-species arising through initiation of transcription from three alternative promoters (pI, pIII and pIV). (**c**) MHC class II expression in WEHI 279.1 B cells infected with LMP vectors containing C2TA-specific hairpin sequences (red) or an empty vector control (blue). GFP^+ cells were stained with a pan-MHCII specific antibody or the respective isotype-control. (**d**) Immunoblot analysis of protein extracts from GFP^+ WEHI 279.1 cells infected with LMP-C2TAsh(6) or empty vector. Data in (**c**) and (**d**) are representative of at least three independent experiments.

Fig. 2 Transgenic expression of the C2TA specific synthetic miRNA in mTECs. (**a**) Diagram of the C2TAkd BAC transgene. The modified miRNA-30 backbone from the vector LMP-C2TAsh(6) was cloned into a BAC transgenic construct containing 152 kilobases of 5' region and 58 kilobases of 3' region flanking the *Aire* gene. In this construct, the *Aire* start codon in exon 1 was replaced by a β-globin intron followed by the miRNA-30-embedded C2TA-specific sequences. (**b**) Relative abundance of the processed synthetic miRNA in purified thymic stromal cells ('immature' $CD80^{lo}$ mTEC, $mTEC^{lo}$; 'mature' $CD80^{hi}$ mTEC, $mTEC^{hi}$; cortical TEC, cTEC; $CD11c^+$ dendritic cells, DC) determined using a custom small RNA TaqMan assay. Values for

mTEC^{lo} were at the lower border of the linear detection range, whereas those for cTECs and DCs were below that threshold and were therefore classified as not detectable (n.d.) (**c**) Relative abundance of Aire mRNA in mTEC subsets defined as in (**b**) determined by quantitative RT-PCR. Data in (**b**) and (**c**) show mean values ± SD of three biological replicates.

Fig. 3 Silencing of C2TA and MHC class II genes in C2TAkd mTECs. (**a**) Relative abundance of the mRNAs encoding for C2TA (left) and a representative C2TA target (the α-chain of H2-A; right) in mTEC subsets (defined as in **Fig. 2b**) determined by quantitative RT-PCR. Data show mean values ± SD of three biological replicates.

(**b**) Microarray expression analysis of MHC class II chains and MHC class II associated C2TA target genes (H2-O, H2-DM and invariant chain (CD74)) in 'mature' (CD80^{hi}) mTECs from wild-type, C2TAkd or C2TA-deficient (*Ciita*$^{-/-}$) mice. Differences between wild-type and C2TAkd were significant; $P < 1\times 10^{-5}$ for all genes except for H2-Eb ($P = 0.003$)). (**c**) Microarray expression analysis of MHC class II unrelated 'putative' C2TA target genes in 'mature' (CD80^{hi}) mTECs from wild-type, C2TAkd or C2TA-deficient (*Ciita*$^{-/-}$) mice ($P > 0.05$ for all genes). Data in (**b**) and (**c**) summarize analyses of three biological replicates ± SD.

Fig. 4 Phenotype, APC-function and 'promiscuous' PTA expression of C2TAkd mTECs. (**a**) Expression of MHC class II on thymic stromal cell subsets of C2TAkd mice (red) as compared to wild-type (blue) or *Ciita*$^{-/-}$ controls (grey) determined by flow cytometry. Conventional (c)DCs were defined according to the surface phenotype CD11c^{hi} CD45RA^{-} and subdivided into intrathymically derived ('autochtonous') cDCs (Sirpα^{-}) or migratory, peripherally derived cDCs (Sirpα^{+}). Plasmacytoid (p)DCs were defined according to the phenotype CD11c^{int} CD45RA^{+}.

(**b**) Immunoblot analysis of MHC class II in mTECs of C2TAkd mice. Because the densitometric values for MHC class II protein (H2-Ea) in $mTEC^{lo}$ were below the threshold of sensitivity, the ratio H2-Ea / Actb is depicted as not defined (ND). Data in (**a**) and (**b**) are representative of at least two independent experiments. (**c**) Dose-response curve of A5 IL-2 GFP-reporter hybridoma cells co-cultured with mTECs from wild-type or C2TAkd mice in the presence of titrated amounts of peptide HA(107-119). The frequency (%) of GFP^+ cells after 17h in co-culture was determined by flow cytometry. Data are representative of two independent experiments (**d**) Frequency of GFP^+ cells ('most mature' $AIRE^+$ mTECs), among total ($CD45^-EpCAM^+Ly51^-$) mTECs from Aire-GFP reporter (Adig) mice in the absence (wild-type) or presence (C2TAkd) of the C2TAkd transgene. The average frequency of GFP^+ cells ± SD is indicated (n = 25 and 11, respectively). (**e**) Distribution of $AIRE^+$ cells in medullary regions of wild-type or C2TAkd thymi. Cryosections were stained for medullary areas (Keratin 5; green) and AIRE (red). The scale bar represents 100 µm. Cortical (C) and medullary (M) areas as well as the cortico-medullary junction (dashed line) are highlighted. Images are representative of at least three organs of each genotype. (**f**) Microarray expression analysis of representative AIRE-dependent and AIRE-independent PTAs in 'mature' ($CD80^{hi}$) mTECs from wild-type and C2TAkd mice. None of the differences were significant ($P > 0.05$ for all genes). Data in (**f**) include three biological replicates.

Fig. 5 Non-redundant contribution of mTECs and hematopoietic APCs to deletional tolerance of $CD4^+$ T cells. (**a**) Thymic profiles in C2TAkd as compared to wild-type mice (5 – 6 mo old). The average frequency of CD4SP cells ± SD is indicated (n = 9 and 10, respectively; $P = 0.001$). The total thymic cellularity was not

different between the two genotypes (not shown). (**b**) Frequency of thymocyte subsets in C2TAkd and wild-type mice. (**c**) Thymic profiles in wild-type or C2TAkd recipients after reconstitution with wild-type or MHCII-KO bone marrow. The average frequency of CD4SP cells ± SEM is indicated (n: WT→WT = 9; WT→C2TAkd = 10; MHCII-KO→WT = 7; MHCII-KO→C2TAkd = 9). (**d**) Summary of the data depicted in (**c**), *P < 0.01 and **P < 0.001.

Fig. 6 Rescue from clonal deletion and increased generation of OVA-specific T_{reg} cells in DO11.10 × Aire-OVA × C2TAkd thymi. (**a**) Relative expression of Aire-OVA transgene in the absence (wild-type) or presence (C2TAkd) of the C2TAkd transgene. The relative mRNA quantity in purified stromal cells ('immature' $CD80^{lo}$ mTEC = $mTEC^{lo}$; 'mature' $CD80^{hi}$ mTEC = $mTEC^{hi}$; $CD11c^+$ dendritic cells = DC) was analyzed by quantitative RT-PCR. Data show the mean relative expression ± SD of three biological replicates. (**b**) Thymocyte subsets in DO11.10 or DO11.10 × Aire-OVA mice in the absence or presence of mTEC-specific C2TA silencing. The average frequency ± SD of CD4SP cells (dot plots) as well as of $DO11.10^+$ cells among gated CD4SP thymocytes (histograms) is indicated. (**c**) Summary of the frequencies of $DO11.10^+$ cells among gated CD4SP thymocytes depicted in (**b**). Total n: DO11.10 = 10; DO11.10 × Aire-OVA = 11; DO11.10 × Aire-OVA × C2TAkd = 14, *P < 0.001. (**d**) Foxp3 expression (intracellular staining) in CD4SP cells in DO11.10, DO11.10 × Aire-OVA and DO11.10 × Aire-OVA × C2TAkd mice. The average frequencies ± SD of $DO11.10^+Foxp3^+$ cells among CD4SP thymocytes are indicated. (**e**) Total number of $DO11.10^+Foxp3^+$ CD4SP thymocytes in DO11.10, DO11.10 × Aire-OVA and DO11.10 × Aire-OVA × C2TAkd mice. Silencing of C2TA in mTECs leads to a significant increase in OVA-specific T_{reg} cells in the presence of cognate

antigen, *$P < 0.001$. (**f**) Total number of DO11.10$^+$Foxp3$^-$ (apparently 'naïve') CD4SP thymocytes in the presence of cognate antigen, *$P < 0.001$.

Fig. 7 Rescue from clonal deletion and increased generation of HA-specific T_{reg} cells in TCR-HA × Aire-HA × C2TAkd thymi. (**a**) Thymocyte subsets in TCR-HA or TCR-HA × Aire-HA mice in the absence or presence of mTEC-specific C2TA silencing. The average frequency ± SD of CD4SP cells (dot plots) and of TCR-HA$^+$ cells among gated CD4SP thymocytes (histograms) is indicated. (**b**) Summary of the frequencies of TCR-HA$^+$ cells among gated CD4SP thymocytes depicted in (**a**). Total n: TCR-HA = 7; TCR-HA × Aire-HA = 6; TCR-HA × Aire-HA × C2TAkd = 14, *$P < 0.001$. (**c**) Foxp3 expression in CD4SP cells. The average frequencies ± SD of TCR-HA$^+$Foxp3$^+$ cells among CD4SP thymocytes are indicated. Expression of Foxp3 was assessed by intracellular staining. (**d**) Total number of TCR-HA$^+$Foxp3$^+$ CD4SP thymocytes. Similar to the observations in the DO11.10 × Aire-OVA model, silencing of C2TA in mTECs leads to a significant increase in HA-specific T_{reg} cells in the presence of cognate antigen. (**e**) Total number of TCR-HA$^+$Foxp3$^-$CD4SP thymocytes in the presence of cognate antigen.

Fig. 8 The C2TAkd mediated 'cell fate conversion' of *DO11*.10 × Aire-OVA thymocytes is independent of cross-presentation by DCs. (**a**) Thymocyte subsets in wild-type, Aire-OVA or Aire-OVA × C2TAkd recipients 6 to 8 weeks after reconstitution with DO11.10 or DO11.10 × ΔDC bone marrow cells. The average frequency ± SD of CD4SP cells (dot plots) and of DO11.10$^+$ cells among gated CD4SP thymocytes (histograms) is indicated. Compared to DO11.10 × ΔDC→Aire-OVA chimeras, DO11.10 × ΔDC→Aire-OVA × C2TAkd chimeras show a significant

increase in DO11.10^{+}CD4^{+} T cells (P = 0.00001). Percentage (**b**) (P = 0.005) and absolute number (**c**) of Foxp3^{+}DO11.10^{+} CD4SP cells resulting from C2TA silencing in AIRE × OVA and Aire-OVA × C2TAkd recipients of DO11.10 × ΔDC bone marrow. (**d**) Total number of DO11.10^{+}Foxp3^{-}CD4SP thymocytes in the presence of cognate antigen. Data are representative of at least 3 chimeras in each group, *P < 0.001.

Methods

Mice. MHCII-KO (*H2-Ab1*$^{-/-}$) [48], *Ciita*$^{-/-}$ [49], TCR-HA [50], DO11.10 [51], Aire-OVA [19], Aire-HA [19], Pgk-HA [33], Adig [29] and ΔDC [3] mice have been described previously. C57BL/6 and BALB/c mice were purchased from Charles River. Mice were maintained in individually ventilated cages. Animal studies were approved by local authorities (Regierung von Oberbayern).

'Designer' miRNA. The MSCV-based LTRmiR30-PIG (LMP) vector was purchased from Open Biosystems. Four 97-mer oligonucleotides (MH3–6) containing 22 bp short hairpin sequences complementary to C2TA (with at least three mismatches to any other gene) were designed using the 'shRNA retriever' resource available at *http://katahdin.cshl.org:9331/homepage/siRNA/RNAi.cgi?type=shRNA*:

MH3: 5′ TGCTGTTGACAGTGAGCGCGGGCCTCCTTGAGTGATACAATAGTGAAG CCACAGATGTATTGTATCACTCAAGGAGGCCCTTGCCTACTGCCTCGGA 3′

MH4: 5′ TGCTGTTGACAGTGAGCGAGCAGCTACCTGGAACTCCTTATAGTGAAG CCACAGATGTATAAGGAGTTCCAGGTAGCTGCCTGCCTACTGCCTCGGA 3′

MH5: 5′ TGCTGTTGACAGTGAGCGAGCCCAGCTACCTTGTACACTTTAGTGAAG CCACAGATGTAAAGTGTACAAGGTAGCTGGGCCTGCCTACTGCCTCGGA 3′

MH6: 5′ TGCTGTTGACAGTGAGCGCGGCTGGCACAGTGCAATGAAATAGTGAAG CCACAGATGTATTTCATTGCACTGTGCCAGCCATGACTACTGCCCGGA 3′

Cloning of these sequences into the LMP vector was performed according to the manufacturer´s protocol.

C2TAkd mice. A construct containing a β-globin intron followed by the recombinant C2TAsh(6) miRNA precursor and a poly-A signal was inserted by homologous

recombination into the mouse BAC RP23-77011 (BACPAC). The targeting vector contained homology boxes spanning nucleotides -379 to -2 (5') and 17 to 399 (3') of the *Aire* gene. A neomycin resistance gene flanked by FRT-sites was used to select successfully recombined clones and was subsequently removed. Transgenic mice were generated by injection of linearized BAC DNA into pronuclei of C57BL/6 × CBA F1 zygotes. Mice were backcrossed to the BALB/c or C57BL/6 background for at least three generations before analysis. For genotyping of C2TAkd mice the following primers were used: forward 5´ TAAATTCTGGCTGGCGTGG 3´ and reverse 5´ ACCGGACTAGTGGAAAAGCGCCTCCCCTACC 3´.

Antibodies and flow cytometry. Fluorescein isothiocyanate (FITC)–conjugated mAb to CD172a (P84), Phycoerythrin (PE)-conjugated mAbs to Ly51 (BP-1), Cy-chrome-conjugated (Cy) mAbs to CD8 (53-6.7), CD45 (Ly-5), CD11c (HL3), phycoerythrin-Cy7 (PE-Cy7)-conjugated streptavidin, mAbs to CD25 (PC61), allophycocyanin-Cy7 (APC-Cy7)-conjugated mAbs to CD4 (GK1.5) and biotin-conjugated monoclonal antibodies (mAbs) to CD8 (53-6.7), CD4 (GK 1.5), CD80 (B7.1, 16-10A1) and CD45RA (14.8) were purchased from Becton Dickinson. Allophycocyanin (APC)-conjugated mAb to EpCAM (G8.8) and to Foxp3 (FJK-16s) were purchased from BioLegend and eBiosciences, respectively. mAbs to TCR-HA (6.5), DO11.10 (KJ1.26) and pan-MHCII (P7.7) were purified from hybridoma supernatant and conjugated to FITC, PE or Alexa647.

Immunofluorescence. 5 µm frozen sections were fixed, washed and blocked with 10% (vol/vol) FCS in PBS, followed by incubation with rabbit anti-keratin 5 antibody (Covance). After washing, sections were incubated with Alexa Fluor 488-conjugated

secondary anti-rabbit antibody (Molecular Probes), blocked with rabbit serum (Jackson ImmunoLaboratories) and incubated with biotin anti-keratin 8 antibody (TROMA-1) (Developmental Studies Hybridoma Bank) or biotin anti-AIRE antibody (5H12-2). Subsequently, sections were washed and incubated with streptavidin-Cy3 (Jackson ImmunoLaboratories). Nuclei were counterstained with ProLong Gold antifade reagent with DAPI (Molecular Probes).

Western analysis. Lysates from 1×10^6 WEHI 279.1 or 3×10^5 thymic stromal cells were run on SDS/PAGE under reducing conditions and transferred onto a polyvinylidene difluoride membrane (Roche). The membrane was blocked with 4 % skim milk in PBS and incubated with mouse anti mouse β-actin (AC-15, Sigma-Aldrich) or rat anti mouse MHCII (H2-Ea) (IBL-5/22, Santa Cruz). The membrane was washed with 0.05 % Tween 20 and incubated with horse radish peroxidase (HRP)-conjugated polyclonal rabbit anti mouse (P260, DAKO) or HRP-conjugated polyclonal mouse anti rat (212-035-168, Dianova). Signal development was performed using Super Signal West Pico (Pierce).

Antigen-presentation assay. 2×10^4 A5 hybridoma cells were co-cultured with 2×10^4 APCs in 200 µl Iscove´s modified Dulbecco´s medium (IMDM) supplemented with 1% FCS. After 17 h, cells were harvested and GFP expression of A5 cells was measured by flow cytometry.

Preparation of thymic stroma. Stromal cells were isolated as described elsewhere [19]. Subsets were sorted according to surface expression of CD45, Ly51, EpCAM, CD11c, CD45RA and Sirpα (CD172a): mTECs = $CD45^-Ly51^-EpCAM^+$; pDCs =

$CD45^+CD11c^{int}CD45RA^+$; Sirpα$^+$ cDCs = $CD45^+CD11c^{high}CD172a^+$; Sirpα$^-$ cDCs = $CD45^+CD11c^{high}CD172a^-$; cTECs = $CD45^-Ly51^+$.

Bone marrow chimeras. Bone marrow was depleted of T cells using biotinylated CD8 and CD4 mAbs and streptavidin MACS beads (Miltenyi Biotech) according to standard procedures. BALB/c or C57BL/6 recipient mice were irradiated with split doses of 2 × 450 rad or 2 × 550 rad, respectively, and reconstituted with 8×10^6 bone marrow cells.

Quantitative PCR. Total RNA was isolated from thymic stromal cells using the miRNAeasy kit including a DNase digest (Qiagen) and reverse transcribed using the iScript cDNA synthesis kit (Biorad). PCR reactions were performed in duplicates on a CFX96 realtime thermal cycler (Biorad) using the myIQ sybrgreen mastermix (Biorad). Primers were: *Actb* 5´ GCCTTCCTTCTTGGGTAT 3´ and 5´ GGCATAGAGGTCTTTACGG 3´, *Aire* 5´ CCTTATCCAGCAGGTGTTT 3´ and 5´ CGGGCCTTGTTCTTCA 3´, *Aire-OVA* transgene 5´ GCTGGGAGGATGAACTATTA 3´ and 5´ CATTGATGCGTTTGAGGT 3´, *H2-Aa* 5´ GGCTCAGAAATAGCAAGTCA 3´ and 5´ AATCTCAGGTTCCCAGTGTT 3´, *Ciita* 5´ CCTATGCCAACATTGCG 3´ and 5´ GGCTTCTGTCCTGCTTCTA 3´. Fluorescence was recorded at the annealing step and relative expression levels were calculated with the comparative Ct method using *Actb* for normalization.

miRNA quantification. A custom small RNA assay for the detection of UUUCAUUGCACUGUGCCAGCCA (mature 'C2TA miRNA') was designed and manufactured by Applied Biosystems. Total RNA was isolated with the miRNAeasy

kit including a DNase digest (QIAGEN). Reverse transcription was performed with primers for small nucleolar RNA (snoRNA202) and the mature 'C2TA miRNA' using the TaqMan microRNA RT kit (Applied Biosystems). PCR reactions were run in duplicate using primer / probe combinations for snoRNA202 and 'C2TA miRNA' (Applied Biosystems) and the TaqMan Universal PCR Master Mix (Applied Biosystems). Fluorescence was recorded at the annealing step and relative expression levels were calculated with the comparative Ct method using snoRNA202 for normalization.

Microarray. Gene expression profiling was performed on Affymetrix Mouse Gene ST 1.0 arrays. RNA was isolated using the miRNAeasy kit (QIAGEN) and labeled using the WT Expression Kit (Affymetrix). Raw data analysis was performed with R (http://www.R-project.org) and Bioconductor [52]. Arrays were assessed for quality and RMA-normalized. The data were analyzed for differential gene expression using an empirical Bayes moderated *t*-test [53], implemented in the Bioconductor package Linear Models for Microarray Data (LIMMA). The results were sorted by the false discovery rate and exported in tab-delimited format.

Statistical analysis. Statistical significance was assessed by the two-tailed Student's *t* test with unequal variance.

References

1. Hogquist, K.A., Baldwin, T.A. & Jameson, S.C. Central tolerance: learning self-control in the thymus. *Nat Rev Immunol* **5**, 772-782 (2005).
2. Klein, L., Hinterberger, M., Wirnsberger, G. & Kyewski, B. Antigen presentation in the thymus for positive selection and central tolerance induction. *Nat Rev Immunol* **9**, 833-844 (2009).
3. Ohnmacht, C. *et al.* Constitutive ablation of dendritic cells breaks self-tolerance of CD4 T cells and results in spontaneous fatal autoimmunity. *J Exp Med* **206**, 549-559 (2009).
4. van Meerwijk, J.P. *et al.* Quantitative impact of thymic clonal deletion on the T cell repertoire. *J Exp Med* **185**, 377-383 (1997).
5. Akiyama, T. *et al.* Dependence of self-tolerance on TRAF6-directed development of thymic stroma. *Science* **308**, 248-251 (2005).
6. Akiyama, T. *et al.* The tumor necrosis factor family receptors RANK and CD40 cooperatively establish the thymic medullary microenvironment and self-tolerance. *Immunity* **29**, 423-437 (2008).
7. Hikosaka, Y. *et al.* The cytokine RANKL produced by positively selected thymocytes fosters medullary thymic epithelial cells that express autoimmune regulator. *Immunity* **29**, 438-450 (2008).
8. Kajiura, F. *et al.* NF-kappa B-inducing kinase establishes self-tolerance in a thymic stroma-dependent manner. *J Immunol* **172**, 2067-2075 (2004).
9. Kinoshita, D. *et al.* Essential role of IkappaB kinase alpha in thymic organogenesis required for the establishment of self-tolerance. *J Immunol* **176**, 3995-4002 (2006).
10. Rossi, S.W. *et al.* RANK signals from CD4(+)3(-) inducer cells regulate development of Aire-expressing epithelial cells in the thymic medulla. *J Exp Med* **204**, 1267-1272 (2007).
11. Mathis, D. & Benoist, C. Aire. *Annu Rev Immunol* **27**, 287-312 (2009).
12. Peterson, P., Org, T. & Rebane, A. Transcriptional regulation by AIRE: molecular mechanisms of central tolerance. *Nat Rev Immunol* **8**, 948-957 (2008).
13. Derbinski, J. *et al.* Promiscuous gene expression in thymic epithelial cells is regulated at multiple levels. *J Exp Med* **202**, 33-45 (2005).
14. Anderson, M.S. *et al.* Projection of an immunological self shadow within the thymus by the aire protein. *Science* **298**, 1395-1401 (2002).
15. Gallegos, A.M. & Bevan, M.J. Central tolerance to tissue-specific antigens mediated by direct and indirect antigen presentation. *J Exp Med* **200**, 1039-1049 (2004).
16. Millet, V., Naquet, P. & Guinamard, R.R. Intercellular MHC transfer between thymic epithelial and dendritic cells. *Eur J Immunol* **38**, 1257-1263 (2008).
17. Koble, C. & Kyewski, B. The thymic medulla: a unique microenvironment for intercellular self-antigen transfer. *J Exp Med* **206**, 1505-1513 (2009).
18. Gray, D., Abramson, J., Benoist, C. & Mathis, D. Proliferative arrest and rapid turnover of thymic epithelial cells expressing Aire. *J Exp Med* **204**, 2521-2528 (2007).
19. Aschenbrenner, K. *et al.* Selection of Foxp3+ regulatory T cells specific for self antigen expressed and presented by Aire+ medullary thymic epithelial cells. *Nat Immunol* **8**, 351-358 (2007).

20. Jordan, M.S. *et al.* Thymic selection of CD4+CD25+ regulatory T cells induced by an agonist self-peptide. *Nat Immunol* **2**, 301-306 (2001).
21. Liston, A. & Rudensky, A.Y. Thymic development and peripheral homeostasis of regulatory T cells. *Curr Opin Immunol* **19**, 176-185 (2007).
22. Irla, M. *et al.* Autoantigen-specific interactions with CD4+ thymocytes control mature medullary thymic epithelial cell cellularity. *Immunity* **29**, 451-463 (2008).
23. Reith, W., LeibundGut-Landmann, S. & Waldburger, J.M. Regulation of MHC class II gene expression by the class II transactivator. *Nat Rev Immunol* **5**, 793-806 (2005).
24. Zeng, Y., Wagner, E.J. & Cullen, B.R. Both natural and designed micro RNAs can inhibit the expression of cognate mRNAs when expressed in human cells. *Mol Cell* **9**, 1327-1333 (2002).
25. Stegmeier, F., Hu, G., Rickles, R.J., Hannon, G.J. & Elledge, S.J. A lentiviral microRNA-based system for single-copy polymerase II-regulated RNA interference in mammalian cells. *Proc Natl Acad Sci U S A* **102**, 13212-13217 (2005).
26. Dickins, R.A. *et al.* Tissue-specific and reversible RNA interference in transgenic mice. *Nat Genet* **39**, 914-921 (2007).
27. Dickins, R.A. *et al.* Probing tumor phenotypes using stable and regulated synthetic microRNA precursors. *Nat Genet* **37**, 1289-1295 (2005).
28. Paddison, P.J. *et al.* Cloning of short hairpin RNAs for gene knockdown in mammalian cells. *Nat Methods* **1**, 163-167 (2004).
29. Gardner, J.M. *et al.* Deletional tolerance mediated by extrathymic Aire-expressing cells. *Science* **321**, 843-847 (2008).
30. Otten, L.A. *et al.* Revisiting the specificity of the MHC class II transactivator CIITA in vivo. *Eur J Immunol* **36**, 1548-1558 (2006).
31. LeibundGut-Landmann, S. *et al.* Mini-review: Specificity and expression of CIITA, the master regulator of MHC class II genes. *Eur J Immunol* **34**, 1513-1525 (2004).
32. Wu, L. & Shortman, K. Heterogeneity of thymic dendritic cells. *Semin Immunol* **17**, 304-312 (2005).
33. Klein, L., Khazaie, K. & von Boehmer, H. In vivo dynamics of antigen-specific regulatory T cells not predicted from behavior in vitro. *Proc Natl Acad Sci U S A* **100**, 8886-8891 (2003).
34. Klein, L., Roettinger, B. & Kyewski, B. Sampling of complementing self-antigen pools by thymic stromal cells maximizes the scope of central T cell tolerance. *Eur J Immunol* **31**, 2476-2486 (2001).
35. Nedjic, J., Aichinger, M., Emmerich, J., Mizushima, N. & Klein, L. Autophagy in thymic epithelium shapes the T-cell repertoire and is essential for tolerance. *Nature* **455**, 396-400 (2008).
36. Oukka, M. *et al.* CD4 T cell tolerance to nuclear proteins induced by medullary thymic epithelium. *Immunity* **4**, 545-553 (1996).
37. Li, J., Park, J., Foss, D. & Goldschneider, I. Thymus-homing peripheral dendritic cells constitute two of the three major subsets of dendritic cells in the steady-state thymus. *J Exp Med* **206**, 607-622 (2009).
38. Proietto, A.I. *et al.* Dendritic cells in the thymus contribute to T-regulatory cell induction. *Proc Natl Acad Sci U S A* **105**, 19869-19874 (2008).
39. Bensinger, S.J., Bandeira, A., Jordan, M.S., Caton, A.J. & Laufer, T.M. Major histocompatibility complex class II-positive cortical epithelium mediates the

selection of CD4(+)25(+) immunoregulatory T cells. *J Exp Med* **194**, 427-438 (2001).
40. Liston, A. *et al.* Differentiation of regulatory Foxp3+ T cells in the thymic cortex. *Proc Natl Acad Sci U S A* **105**, 11903-11908 (2008).
41. Spence, P.J. & Green, E.A. Foxp3+ regulatory T cells promiscuously accept thymic signals critical for their development. *Proc Natl Acad Sci U S A* **105**, 973-978 (2008).
42. Wirnsberger, G., Mair, F. & Klein, L. Regulatory T cell differentiation of thymocytes does not require a dedicated antigen-presenting cell but is under T cell-intrinsic developmental control. *Proc Natl Acad Sci U S A* **106**, 10278-10283 (2009).
43. Lio, C.W. & Hsieh, C.S. A two-step process for thymic regulatory T cell development. *Immunity* **28**, 100-111 (2008).
44. Bautista, J.L. *et al.* Intraclonal competition limits the fate determination of regulatory T cells in the thymus. *Nat Immunol* **10**, 610-617 (2009).
45. Leung, M.W., Shen, S. & Lafaille, J.J. TCR-dependent differentiation of thymic Foxp3+ cells is limited to small clonal sizes. *J Exp Med* **206**, 2121-2130 (2009).
46. Derbinski, J., Pinto, S., Rosch, S., Hexel, K. & Kyewski, B. Promiscuous gene expression patterns in single medullary thymic epithelial cells argue for a stochastic mechanism. *Proc Natl Acad Sci U S A* **105**, 657-662 (2008).
47. Venanzi, E.S., Melamed, R., Mathis, D. & Benoist, C. The variable immunological self: genetic variation and nongenetic noise in Aire-regulated transcription. *Proc Natl Acad Sci U S A* **105**, 15860-15865 (2008).
48. Grusby, M.J., Johnson, R.S., Papaioannou, V.E. & Glimcher, L.H. Depletion of CD4+ T cells in major histocompatibility complex class II-deficient mice. *Science* **253**, 1417-1420 (1991).
49. Chang, C.H., Guerder, S., Hong, S.C., van Ewijk, W. & Flavell, R.A. Mice lacking the MHC class II transactivator (CIITA) show tissue-specific impairment of MHC class II expression. *Immunity* **4**, 167-178 (1996).
50. Kirberg, J. *et al.* Thymic selection of CD8+ single positive cells with a class II major histocompatibility complex-restricted receptor. *J Exp Med* **180**, 25-34 (1994).
51. Murphy, K.M., Heimberger, A.B. & Loh, D.Y. Induction by antigen of intrathymic apoptosis of CD4+CD8+TCRlo thymocytes in vivo. *Science* **250**, 1720-1723 (1990).
52. Gentleman, R.C. *et al.* Bioconductor: open software development for computational biology and bioinformatics. *Genome Biol* **5**, R80 (2004).
53. Smyth, G.K. Linear models and empirical bayes methods for assessing differential expression in microarray experiments. *Stat Appl Genet Mol Biol* **3**, Article3 (2004).

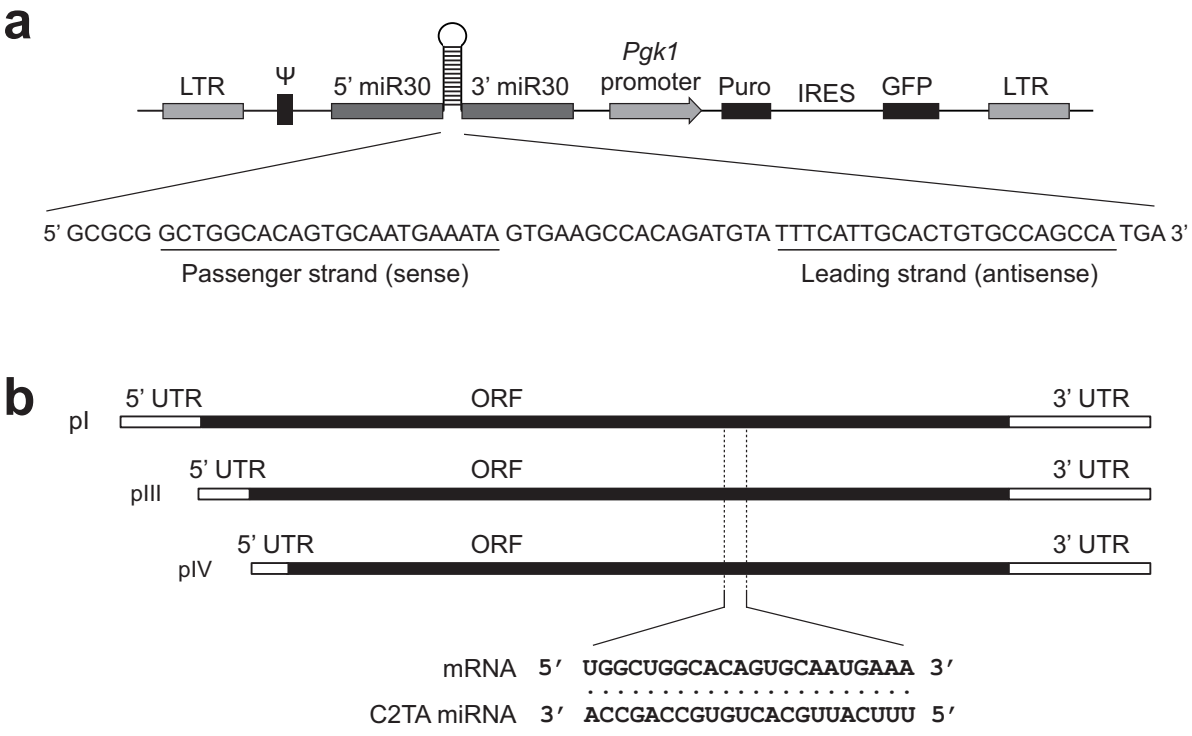
a
LTR
Ψ
5' miR30
3' miR30
Pgk1
promoter
Puro
IRES
GFP
LTR
5' GCGCG GCTGGCACAGTGCAATGAAATA GTGAAGCCACAGATGTA TTTCATTGCACTGTGCCAGCCA TGA 3'
Passenger strand (sense)
Leading strand (antisense)
b
pI
5' UTR
ORF
3' UTR
pIII
5' UTR
ORF
3' UTR
pIV
5' UTR
ORF
3' UTR
mRNA 5′ UGGCUGGCACAGUGCAAUGAAA 3′
C2TA miRNA 3′ ACCGACCGUGUCACGUUACUUU 5′
c
Empty vector
C2TAsh(6)
Isotype control
Events (% max)
100
80
60
40
20
0
10^0
10^1
10^2
10^3
10^4
MHCII
d
Empty vector
C2TAsh(6)
MHCII (H2-Ea)
Actb

Figure 1

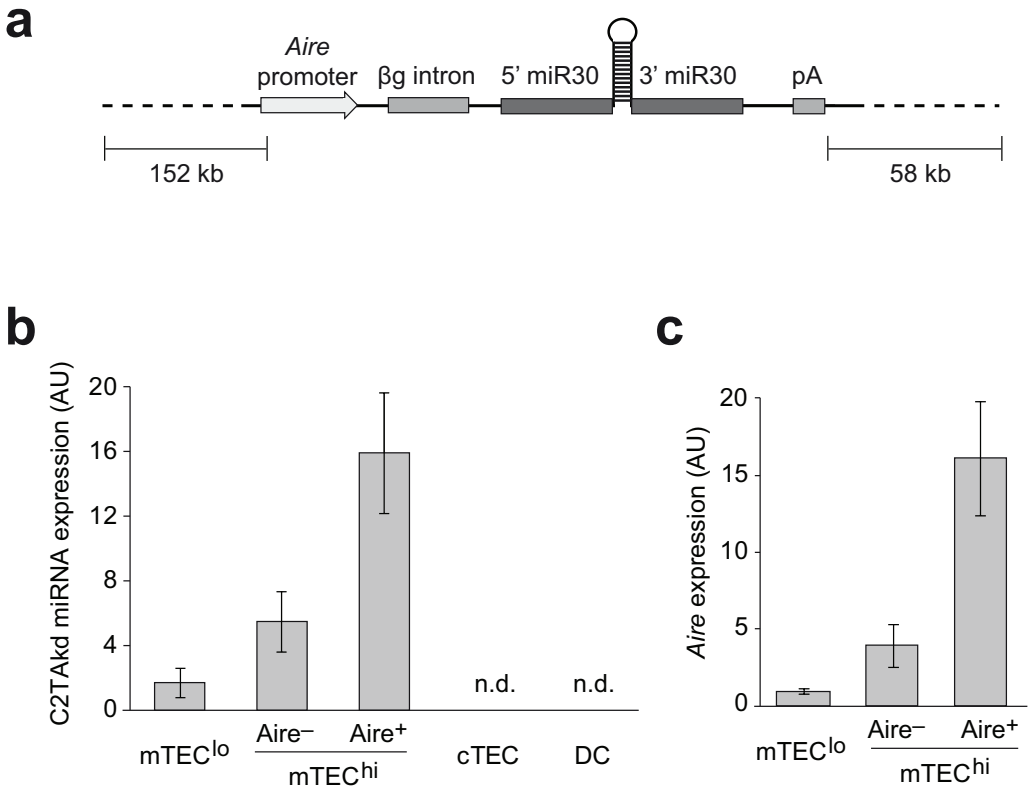
a
Aire
promoter
βg intron
5' miR30
3' miR30
pA
152 kb
58 kb
b
C2TAkd miRNA expression (AU)
20
16
12
8
4
0
n.d.
n.d.
mTEC^lo
Aire–
Aire+
mTEC^hi
cTEC
DC
c
Aire expression (AU)
20
15
10
5
0
mTEC^lo
Aire–
Aire+
mTEC^hi

Figure 2

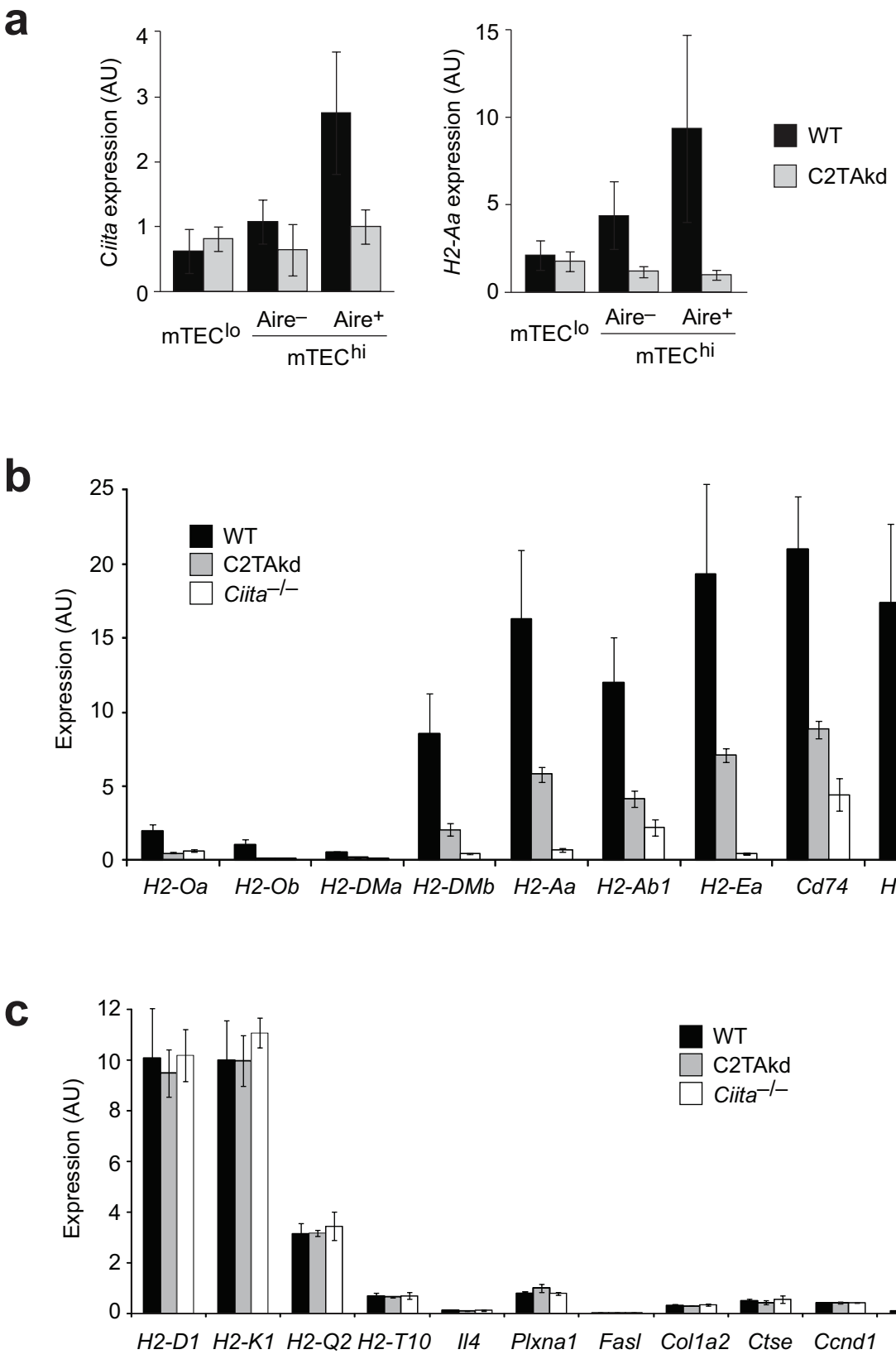
a
Ciita expression (AU)
H2-Aa expression (AU)
WT
C2TAkd
mTEClo
Aire–
Aire+
mTEChi
b
Expression (AU)
WT
C2TAkd
Ciita–/–
H2-Oa
H2-Ob
H2-DMa
H2-DMb
H2-Aa
H2-Ab1
H2-Ea
Cd74
H2-Eb1
c
Expression (AU)
WT
C2TAkd
Ciita–/–
H2-D1
H2-K1
H2-Q2
H2-T10
Il4
Plxna1
Fasl
Col1a2
Ctse
Ccnd1
Il10

Figure 3

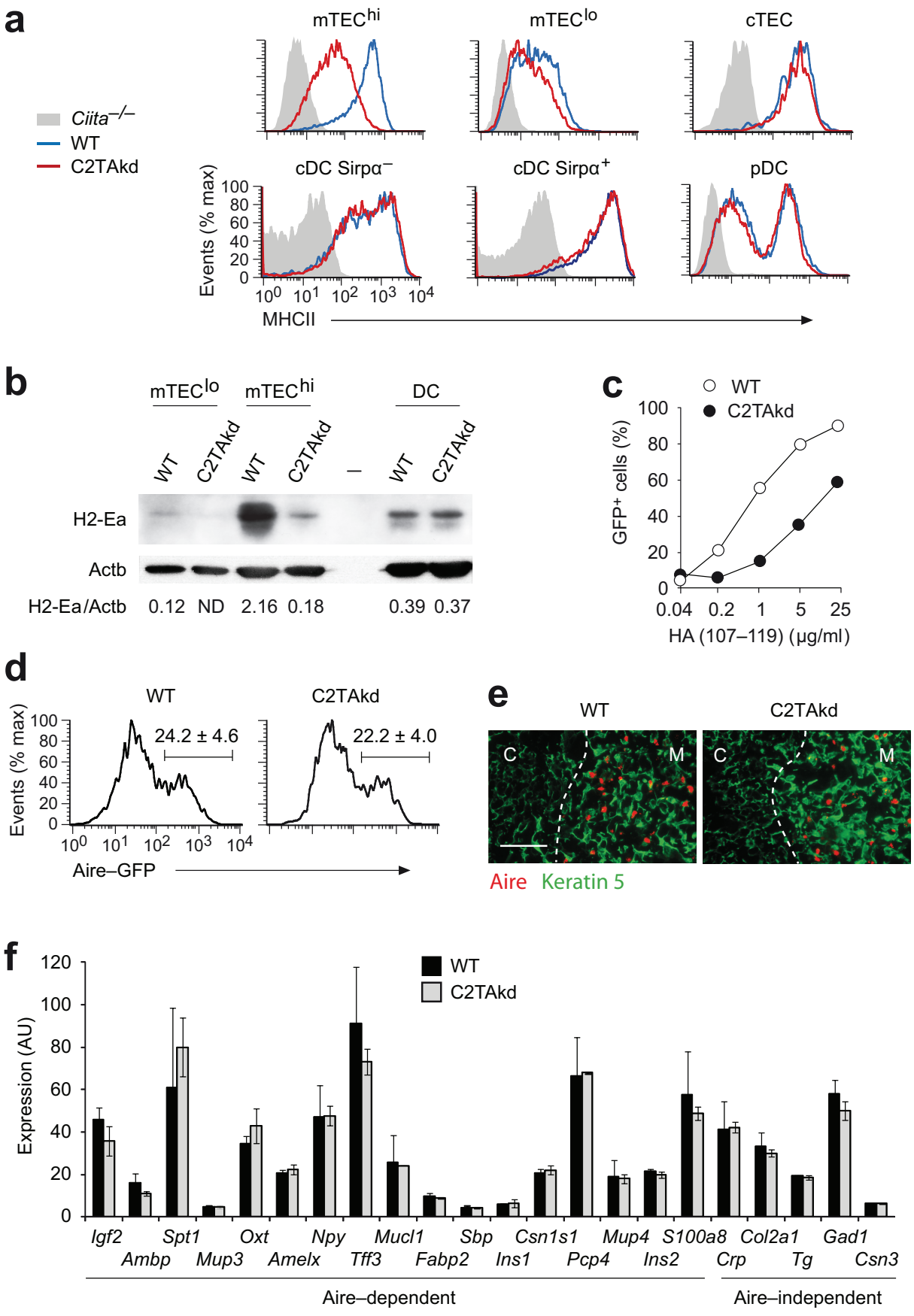
a
Ciita−/−
WT
C2TAkd
mTEChi
mTEClo
cTEC
cDC Sirpα−
cDC Sirpα+
pDC
Events (% max)
MHCII
b
mTEClo
mTEChi
DC
WT
C2TAkd
H2-Ea
Actb
H2-Ea/Actb
0.12 ND 2.16 0.18 0.39 0.37
c
WT
C2TAkd
GFP+ cells (%)
HA (107–119) (μg/ml)
d
WT
C2TAkd
24.2 ± 4.6
22.2 ± 4.0
Events (% max)
Aire–GFP
e
WT
C2TAkd
C
M
Aire Keratin 5
f
WT
C2TAkd
Expression (AU)
Igf2 Ambp Spt1 Mup3 Oxt Amelx Npy Tff3 Mucl1 Fabp2 Sbp Ins1 Csn1s1 Pcp4 Mup4 Ins2 S100a8 Crp Col2a1 Tg Gad1 Csn3
Aire–dependent
Aire–independent

Figure 4

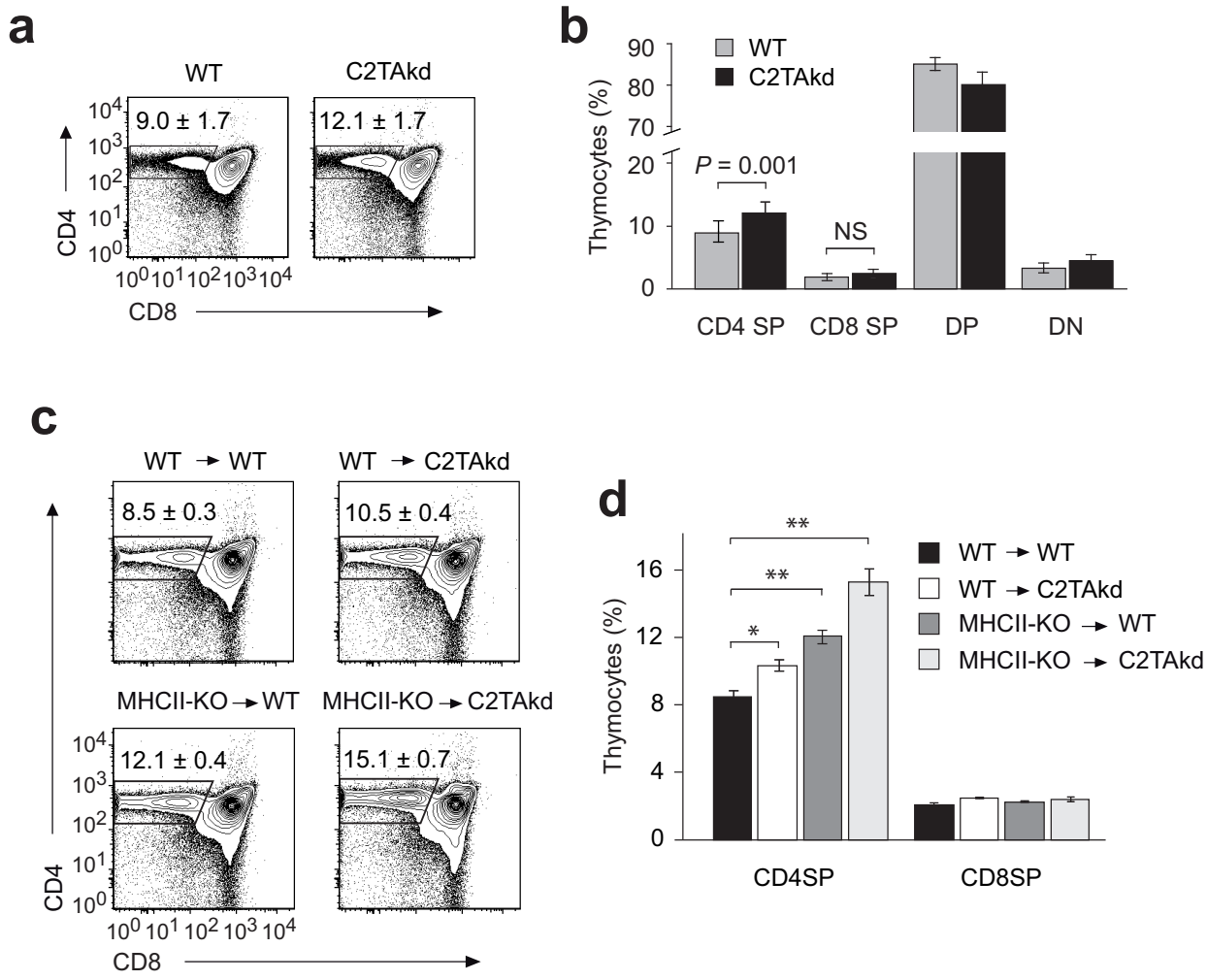
a
WT
C2TAkd
9.0 ± 1.7
12.1 ± 1.7
CD4
CD8
b
WT
C2TAkd
Thymocytes (%)
P = 0.001
NS
CD4 SP
CD8 SP
DP
DN
c
WT → WT
WT → C2TAkd
8.5 ± 0.3
10.5 ± 0.4
MHCII-KO → WT
MHCII-KO → C2TAkd
12.1 ± 0.4
15.1 ± 0.7
CD4
CD8
d
WT → WT
WT → C2TAkd
MHCII-KO → WT
MHCII-KO → C2TAkd
Thymocytes (%)
CD4SP
CD8SP

Figure 5

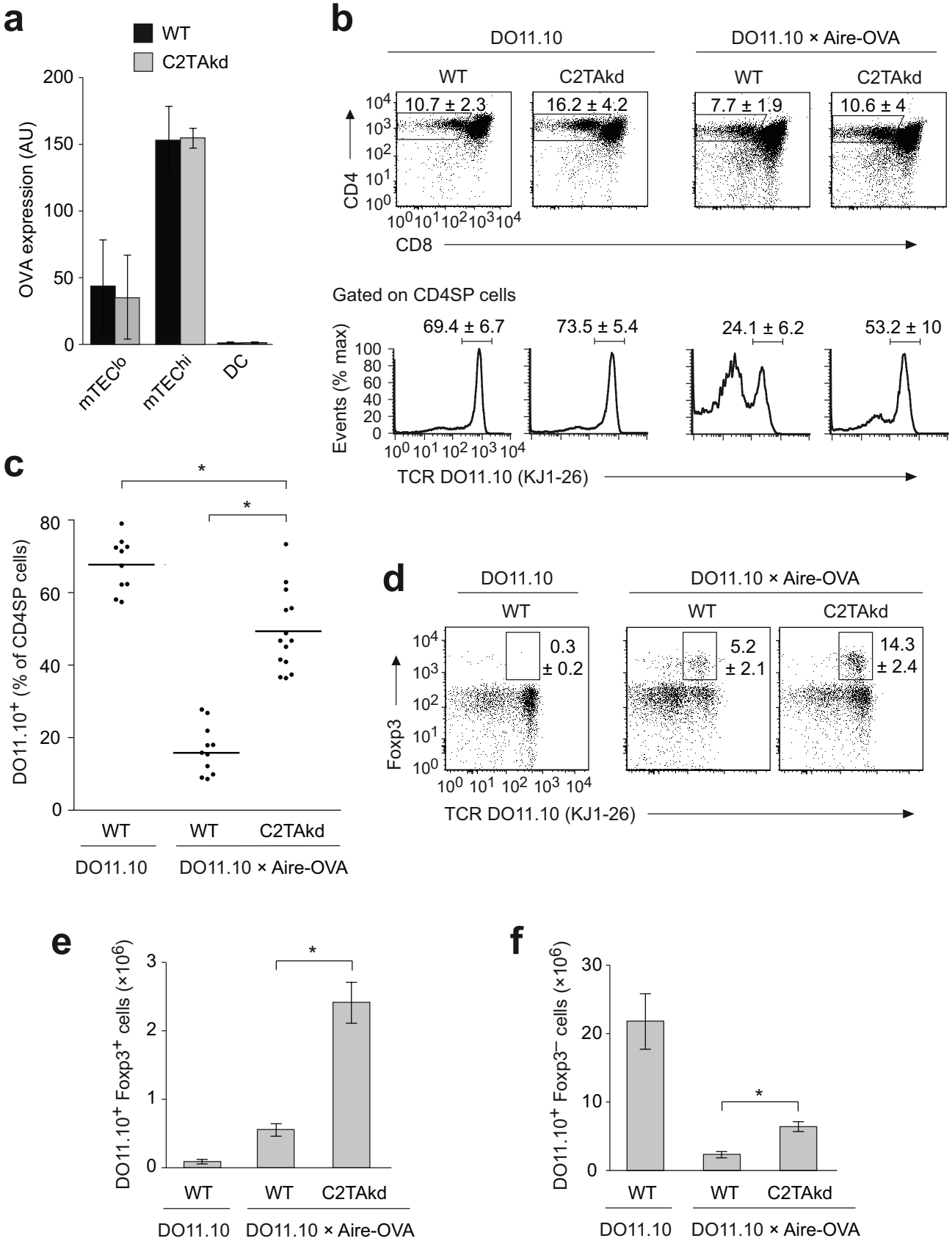
a
WT
C2TAkd
OVA expression (AU)
200
150
100
50
0
mTEClo
mTEChi
DC
b
DO11.10
DO11.10 × Aire-OVA
WT
C2TAkd
WT
C2TAkd
10.7 ± 2.3
16.2 ± 4.2
7.7 ± 1.9
10.6 ± 4
CD4
CD8
Gated on CD4SP cells
69.4 ± 6.7
73.5 ± 5.4
24.1 ± 6.2
53.2 ± 10
Events (% max)
TCR DO11.10 (KJ1-26)
c
DO11.10+ (% of CD4SP cells)
WT
WT
C2TAkd
DO11.10
DO11.10 × Aire-OVA
d
DO11.10
DO11.10 × Aire-OVA
WT
WT
C2TAkd
0.3 ± 0.2
5.2 ± 2.1
14.3 ± 2.4
Foxp3
TCR DO11.10 (KJ1-26)
e
DO11.10+ Foxp3+ cells (×10^6)
WT
WT
C2TAkd
DO11.10
DO11.10 × Aire-OVA
f
DO11.10+ Foxp3− cells (×10^6)
WT
WT
C2TAkd
DO11.10
DO11.10 × Aire-OVA

Figure 6

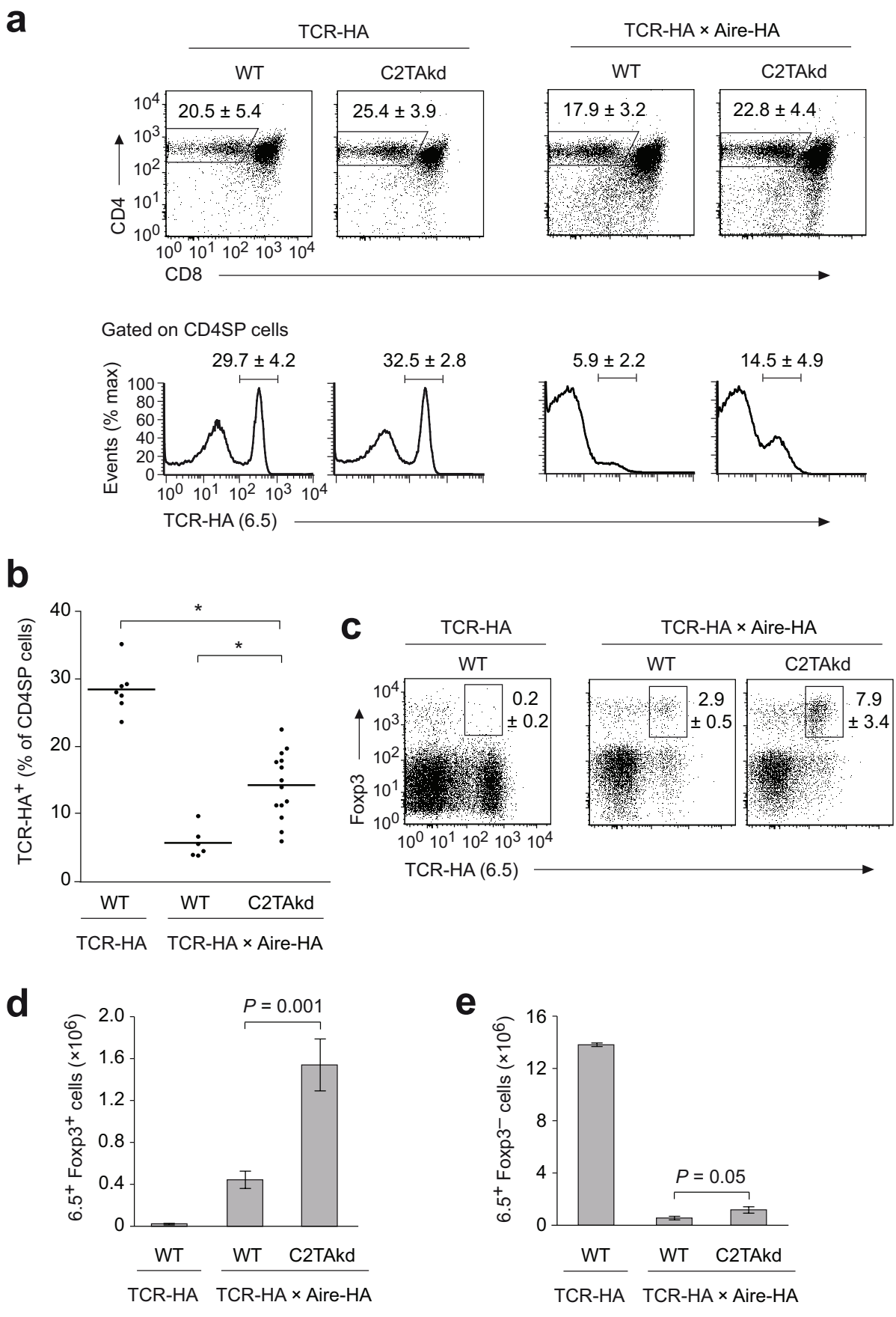
a
TCR-HA
TCR-HA × Aire-HA
WT
C2TAkd
WT
C2TAkd
20.5 ± 5.4
25.4 ± 3.9
17.9 ± 3.2
22.8 ± 4.4
CD4
CD8
Gated on CD4SP cells
29.7 ± 4.2
32.5 ± 2.8
5.9 ± 2.2
14.5 ± 4.9
Events (% max)
TCR-HA (6.5)
b
TCR-HA+ (% of CD4SP cells)
WT
WT
C2TAkd
TCR-HA
TCR-HA × Aire-HA
c
TCR-HA
TCR-HA × Aire-HA
WT
WT
C2TAkd
0.2 ± 0.2
2.9 ± 0.5
7.9 ± 3.4
Foxp3
TCR-HA (6.5)
d
P = 0.001
6.5+ Foxp3+ cells (×10^6)
WT
WT
C2TAkd
TCR-HA
TCR-HA × Aire-HA
e
6.5+ Foxp3− cells (×10^6)
P = 0.05
WT
WT
C2TAkd
TCR-HA
TCR-HA × Aire-HA

Figure 7

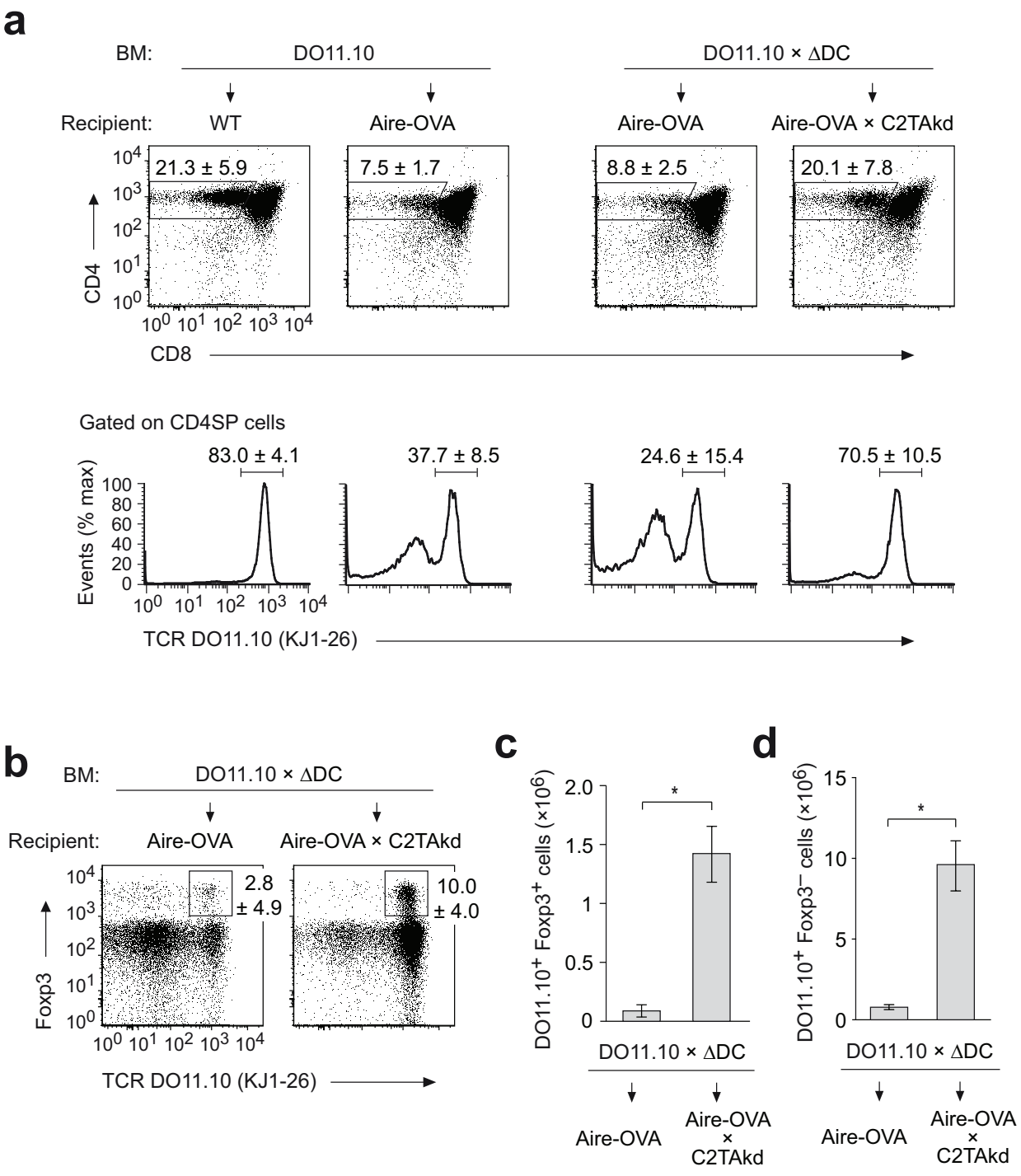
a
BM:
DO11.10
DO11.10 × ΔDC
Recipient:
WT
Aire-OVA
Aire-OVA
Aire-OVA × C2TAkd
21.3 ± 5.9
7.5 ± 1.7
8.8 ± 2.5
20.1 ± 7.8
CD4
CD8
Gated on CD4SP cells
83.0 ± 4.1
37.7 ± 8.5
24.6 ± 15.4
70.5 ± 10.5
Events (% max)
TCR DO11.10 (KJ1-26)
b
BM:
DO11.10 × ΔDC
Recipient:
Aire-OVA
Aire-OVA × C2TAkd
2.8 ± 4.9
10.0 ± 4.0
Foxp3
TCR DO11.10 (KJ1-26)
c
DO11.10+ Foxp3+ cells (×10^6)
DO11.10 × ΔDC
Aire-OVA
Aire-OVA × C2TAkd
d
DO11.10+ Foxp3− cells (×10^6)
DO11.10 × ΔDC
Aire-OVA
Aire-OVA × C2TAkd

Figure 8